Journal of Alloys and Compounds 505 (2010) 273–277

Contents lists available at ScienceDirect

Journal of Alloys and Compounds

journal homepage: www.elsevier.com/locate/jallcom

Application of spark plasma sintering to processing of dense $Ba(Ti_{1-x}Sn_x)O_3$ ($x = 0.13$) ceramic

Gheorghe Aldica[a,*], Marin Cernea[a], Roxana Radu[a], Roxana Trusca[b]

[a] National Institute of Materials Physics, Str. Atomistilor 105 Bis, RO-77125, P.O. BOX: MG-7, Magurele-Bucharest, Romania
[b] METAV-R&D S. A., P.O. 22, Bucharest, Romania

ARTICLE INFO

Article history:
Received 31 March 2010
Received in revised form 1 June 2010
Accepted 10 June 2010
Available online 18 June 2010

Keywords:
Sn-doped $BaTiO_3$
Spark-plasma-sintering technique
Dielectric properties

ABSTRACT

Short time spark plasma sintering at 1200 °C for 10 min and under a uniaxial pressure of 95 MPa followed by annealing at 1100 °C for 5 h is proposed for synthesis of high density (99%) $Ba(Ti_{0.87}Sn_{0.13})O_3$ ceramic. Starting powder of 450 nm was obtained by co-precipitation, while the average grain size in the sintered ceramic was of 580 nm. X-ray diffraction analysis of the as prepared $Ba(Ti_{0.87}Sn_{0.13})O_3$ samples indicated the presence of single phase $BaTi_{0.87}Sn_{0.13}O_3$ developed in the $BaTiO_3$ cubic structure. Samples have high relative dielectric constant of 5680 and low dissipation factor ($\tan\delta = 0.009$) at Curie temperature of 57 °C and 1 kHz, good tunability and ferroelectric properties. Remarkable is that these results are from some points of view different than for the conventionally processed samples with similar stoichiometry. Some ideas in this regard are presented and this suggests that SPS can be useful for expanded possibilities in the control of the properties.

1. Introduction

Solid solutions $Ba(Ti_{1-x}Sn_x)O_3$ (denoted as BTS_x hereafter) show ferroelectric properties and are used for capacitors, relaxors, dielectric amplifier, switching circuit snubbers and sensor [1–7]. BTS_x is also important for practical applications in functionally graded materials [8].

The advantages of the isovalent Sn-substitution at titanium site in BTS_x are related to the possibility to control the dielectric characteristics [9–11]. It is usually observed that the phase transition of BTS_x becomes increasingly diffuse [9], as displayed by significant deviations from the Curie–Weiss law of the temperature dependent permittivity reported for $x > 0.05$ [10]. Broadening of the peak of the dielectric constant, ε_r, in a wide working temperature range [12] is accompanied by enhancement of its level, and both being useful for applications (e.g. capacitors). In addition, with increasing Sn content, the Curie temperature of the paraelectric–ferroelectric phase transition decreases considerably. When $x \leq 0.30$, the Curie temperature of $Ba(Ti_{1-x}Sn_x)O_3$ declines about 8 °C for every 1 at.% of titanium (Ti^{4+}) substitution by tin (Sn^{4+}) [13], so that, e.g., it is about 40 °C for BTS_{13} [11,14]. The ferroelectric domain-structure was observed for $Ba(Ti_{1-x}Sn_x)O_3$, $x \leq 0.13$ [11]. $Ba(Ti_{1-x}Sn_x)O_3$, $x \geq 0.2$ revealed characteristic features of ferroelectric relaxor [10,15].

Apart from the chemical Ti/Sn composition, temperature stability of electric properties strongly depends on the oxygenation level, grain size, grain size distribution and on the presence of certain grain boundaries. Use of fine powders as precursors in combination with spark-plasma-sintering (SPS) is thought to be convenient in order to have a better control of the indicated parameters. It is in general observed that SPS due to specifics of pulsed electrical field application, namely a cleaning process at the surface of the grains [16,17] and enhanced electro-diffusion, can result into significant decrease of the processing times and temperatures [18]. Such effects combined with the use of a uniaxial pressure during SPS-processing can produce ceramics of high density and can preserve or control the grain size and to some extent the grain boundaries. Noteworthy, SPS is also a process with features far from equilibrium, e.g. it involves occurrence of hot spots and much debated plasma states, leading to non homogeneities and defects. Up to now, SPS was used with good results for sintering of $BaTiO_3$ [19–21] ceramics starting from powders produced by solid-state reaction between oxides and carbonates. In this paper, we used SPS to obtain single phase solid solution $Ba(Ti_{1-x}Sn_x)O_3$ ($x = 0.13$) as a high density ceramic. We used powders obtained by co-precipitation. The dielectric and ferroelectric properties of the resulting SPS-processed BTS_{13} ceramic are characterized. We try to

* Corresponding author. Tel.: +40 213690170; fax: +40 213690177.
E-mail address: aldica@infim.ro (G. Aldica).

0925-8388/$ – see front matter © 2010 Elsevier B.V. All rights reserved.
doi:10.1016/j.jallcom.2010.06.044

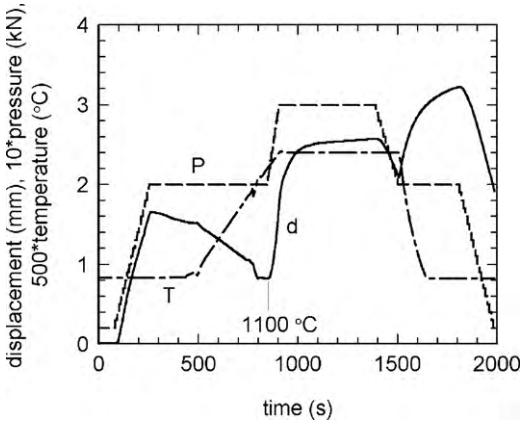

Fig. 1. Displacement (shrinkage), its rate and operating current vs. temperature for BTS_{13} sample.

discuss some specific details of our SPS samples vs. literature data for similar samples obtained by conventional methods.

2. Experimental procedure

The BTS_{13} powder obtained by co-precipitation [22] was sintered by SPS (FCT Systeme GmbH, Germany) at 1200 °C, for 10 min into discs with thickness of 2.35 mm and diameter of 20 mm. A pyrometer measured the temperature. The heating rate was chosen at 100 °C min^{-1} and the applied mechanical uniaxial pressure was 95 MPa. Temperature was taken at 2 mm above the sample on the punch surface, and through an axial hole made in the punch. Sintering was performed in vacuum (30–40 Pa). In the SPS apparatus a current pulsed pattern was applied. The waveform is not square and, in fact, is composed of several spikes (pulses) separated by a current-free interval. Each pulse has the same period of about 3×10^{-3} s. In the current work, a pattern of 12:2 on:off pulses was applied. The total time of one sequence (cycle) is about 0.04 s. The operating parameters, namely voltage and the peak current were below 5 V and 1600 A, respectively. In Fig. 1 is shown the variation of displacement (D), temperature (T), and mechanical pressure (P), as a function of time, during the SPS processing of BTS_{13} powder. The onset temperature of the densification process was 1100 °C and the densification completion is placed above 1200 °C.

After SPS processing, the surface of the bulk BTS_{13} samples was contaminated with carbon from the graphite foils inserted between the die, punches and the ceramic powder. Graphite-layer was mechanically removed. In the volume, samples were dark blue due to the reducing sintering atmosphere used during SPS (low vacuum). In this way, some Ti^{4+} is reduced to Ti^{3+}, a well-known phenomena in SPS sintering [19]. To restore the oxygen stoichiometry and to remove the carbon contamination, SPS dense pellets were annealed in oxygen, at 1100 °C for 5 h.

Microstructure of the samples was investigated using a Hitachi S2600N scanning electron microscope.

Structural characterization of the BTS_{13} precursor powders and sintered ceramics was performed by X-ray diffraction technique using a Bruker-AXS tip D8 ADVANCE diffractometer ($CuK\alpha_1$ radiation, 1.5406 Å). Apparent densities of the sintered pellets were determined by Archimedes method (in water) using a density balance.

Silver paste used as the electrodes, was screen-printed on both surfaces of BTS_{13} pellets. The temperature dependence of the dielectric constant and of the dielectric losses was evaluated in the temperature range from −20 to 225 °C at 1, 10 and 100 kHz by an Agilent 4263B LCR meter equipped with a thermostat. The electrical measurements were carried out in the metal–ferroelectric–metal (MFM) configuration where M is silver and F is the ferroelectric sample ($Ba(Ti_{0.87}Sn_{0.13})O_3$).

P–E loops were measured using aixACCT System with a modular designed electrical characterization system: the TF Analyzer 2000HS series. The dependence of the polarization P on an alternating electric field E with the amplitude of 5 kV/mm was measured at a frequency of 100 Hz with the aid of a Sawyer–Tower circuit. A triangular waveform was chosen for the electric field cycle.

3. Results

3.1. Microstructure

The SEM micrograph of BTS_{13} starting powders shows agglomerates consisting of well crystallized grains with size of 300–600 nm (Fig. 2(a)).

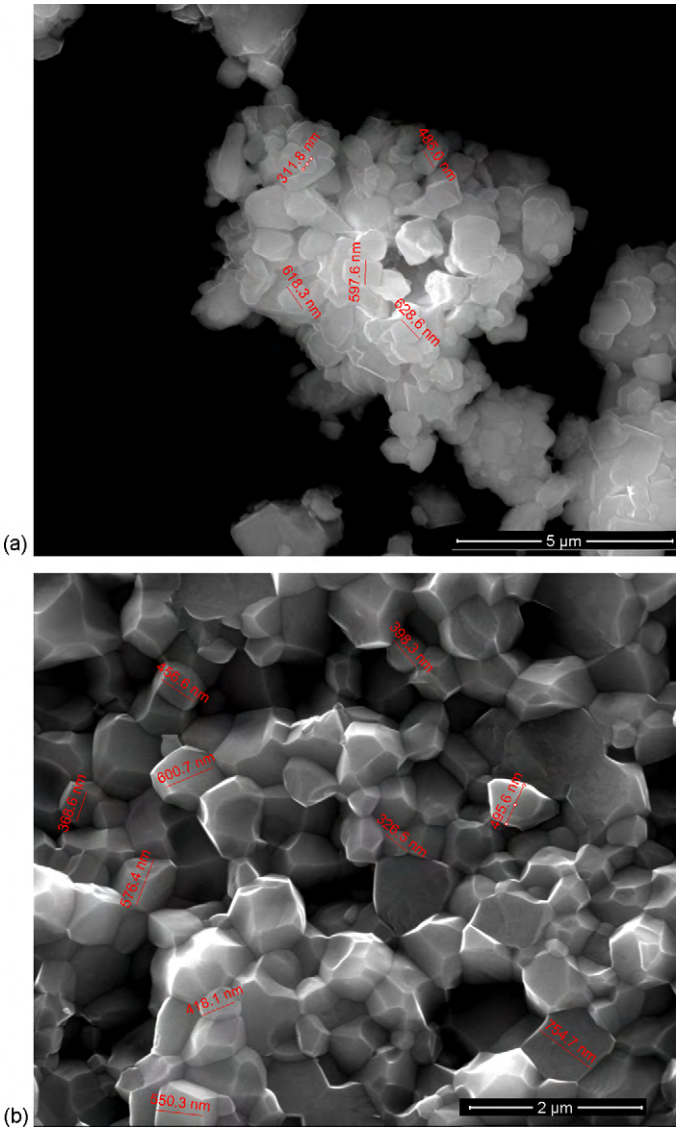

Fig. 2. Scanning electron microscope photomicrographs of the $BaTi_{1-x}Sn_xO_3$, $x = 0.13$ powder (a) and sintered pellets (b).

SEM image of the fractured surface of the annealed pellets are shown in Fig. 2(b). The SPS pellets consist of submicron grains (400–800 nm). This result indicates, as expected, that the short sintering period is an essential factor to obtain fine-grained BTS_{13} ceramics by the SPS process. Some pores located at grain boundaries can be observed. The apparent density of the pellets sintered by SPS technique and annealed at 1100 °C, 5 h in oxygen was about 99% of the theoretical value (6.19 g/cm^3, [23]) of $Ba(Ti_{0.87}Sn_{0.13})O_3$.

3.2. X-ray patterns

Fig. 3 shows the XRD patterns of $BaTi_{1-x}Sn_xO_3$, $x = 0.13$ pellets obtained by SPS and annealed at 1100 °C, 5 h in oxygen.

XRD data of SPS compacted and annealed BTS_{13} pellets, (Fig. 3) indicate that the crystalline structure of the SPS pellets consist of cubic phase (XRD pattern PDF 79-2263) [24]. No secondary phase is observed.

3.3. Dielectric properties

The behaviour of relative permittivity (ε_r) and of tan δ with temperature, at various frequencies (1, 10 and 100 kHz), for the BTS_{13} pellets, is shown in Figs. 4 and 5.

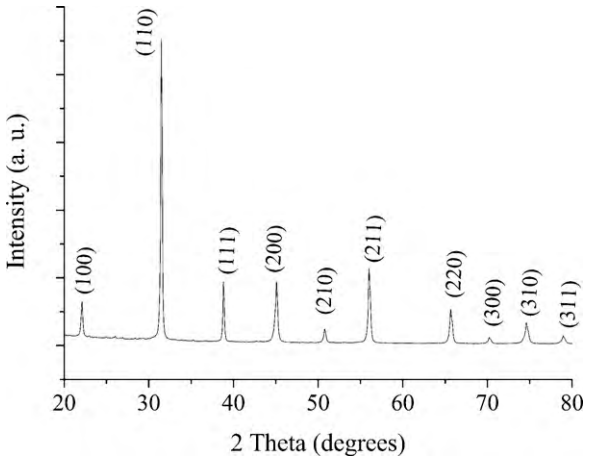

Fig. 3. X-ray diffraction patterns of the $BaTi_{1-x}Sn_xO_3$, $x = 0.13$ pellets obtained by SPS and annealed at 1100 °C, 5 h in oxygen.

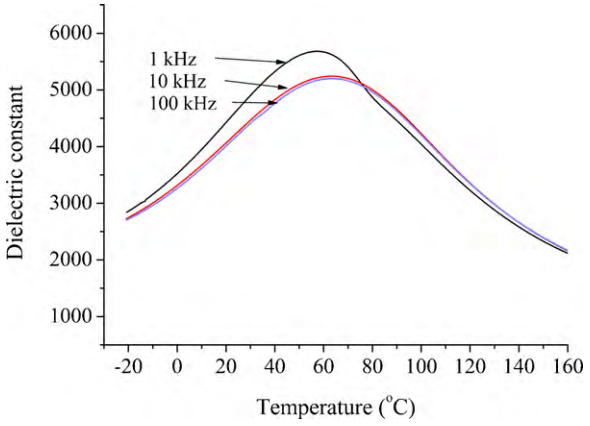

Fig. 4. Temperature dependence of dielectric constant at various frequencies of $Ba(Ti_{0.87}Sn_{0.13})O_3$ ceramic.

There are permittivity peaks for the samples corresponding to their ferroelectric to paraelectric phase transition. The dielectric constants of $Ba(Ti_{0.87}Sn_{0.13})O_3$ pellets were 5680 at 1 kHz, 5240 at 10 kHz and 5200 at 100 kHz, at the Curie temperatures (Figs. 4 and 5). The dielectric maximum shifted to higher temperature for a higher frequency. The Curie temperatures (T_c) were 57, 63 and 64 °C, respectively. Peaks are broad indicating that the phase transition region is diffused. More precise, the full width of half maximum (FWHM) extends to about 78, 87 and 87 °C, at the experimental frequencies (1, 10 and 100 kHz). Dielectric losses tangent (δ) of $Ba(Ti_{0.87}Sn_{0.13})O_3$ pellets were 0.009 at 1 kHz, 0.008 at 10 kHz and 0.004 at 100 kHz, at the Curie temperatures (Figs. 4 and 5). The values of the dielectric characteristics of $BaTi_{0.87}Sn_{0.13}O_3$ ceramics, consolidated by spark plasma sintering, are comparable with the literature data [22,25], and are suitable for applications in, e.g., capacitors.

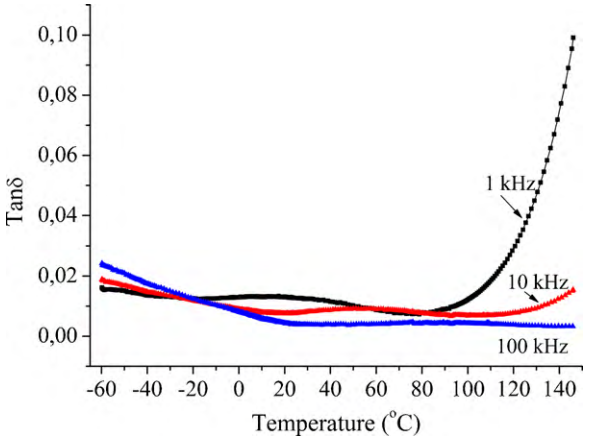

Fig. 5. Temperature dependence of loss tangent (δ) at 1–100 kHz frequencies of $Ba(Ti_{0.87}Sn_{0.13})O_3$ ceramic.

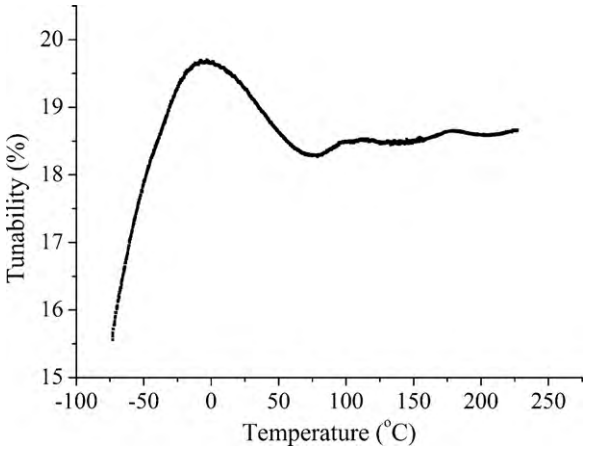

Fig. 6. Tunability at 100 kHz frequency, of $Ba(Ti_{0.87}Sn_{0.13})O_3$ ceramic pellets.

The tunability (=$[\varepsilon(0) - \varepsilon(E)]/\varepsilon(0)$) of $Ba(Ti_{0.87}Sn_{0.13})O_3$ SPS sintered ceramic pellets is shown in Fig. 6.

The tunability at 5 V/cm and 100 kHz frequency, of $Ba(Ti_{0.87}Sn_{0.13})O_3$ sintered pellets showed a monotonic decrease from 19.37% at 20 °C to 18.29% at 79 °C. This result implies that our ceramic is suitable for tunable device applications such as voltage-controlled oscillators, tunable filters and phase shifters.

The ferroelectric characteristics of $Ba(Ti_{0.87}Sn_{0.13})O_3$ ceramic pellets are shown in Fig. 7.

With increasing temperature from 20 to 40 °C, the well-saturated square Polarization (P)–Electric field (E) hysteresis loop becomes large. The values of the coercitive field, E_c, and the remanent polarization, P_r, are shown in Table 1.

As it can be seen in Table 1, the values of E_c and P_r indicate a very small variation with temperature in 20–40 °C range of BTS_{13} ferroelectric characteristics. The E_c and P_r values of our $Ba(Ti_{0.87}Sn_{0.13})O_3$ SPS-ceramic are close to that of $BaTiO_3$ sol–gel bulk ceramic [26].

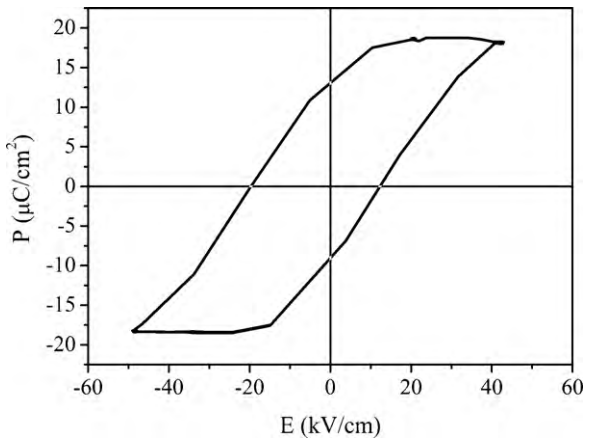

Fig. 7. P–E hysteresis loop at 20 °C, of $Ba(Ti_{0.87}Sn_{0.13})O_3$ ceramic pellets.

Table 1
E_c and P_r values at various temperatures (20, 30 and 40 °C) of $Ba(Ti_{0.87}Sn_{0.13})O_3$ ceramic pellets.

Temperature (°C)	E_c (kV/cm)	P_r (μC/cm^2)
20	12.3	13.07
30	19.1	13.57
40	19.9	13.76

4. Discussion

Barium stanate titanate is considered a prototype of a ferroelectric material with diffused phase transition. The physical mechanism of diffuse-type phase transition has various reasons. Smolensky [9] and Kvyatkovskii [27] proposed that the broadened phase transition originates from the chemical composition fluctuation and the distribution of defects. More precisely, the temperature range of the diffuse ferroelectric phase transition and the value of the shift of the average transition temperature are a function of the degree of disorder and chemical composition. Isupov [28,29] explained some problems of ferroelectrics with diffused phase transition in view of polar region. Another factor that can contribute to broadening of the ferroelectric transition in real samples it refers to nonuniform internal and external stresses [30]. These factors are directly related to the technology of preparation and processing of samples.

Though many factors can reduce the nonlinear dielectric response, there are two in the current system that are believed to predominate. The first is a scaling effect associated with an average grain size decrease. The second is an increase in the number and/or features of domain wall pinning sites. An important processing goal is to obtain high-quality microstructure with desired grain size and density. One related aspect is that ionic conductivity in BTS_x occurs due to the migration of O^{2-} ions through oxygen vacancies. In our case, SPS is responsible for smaller average grain size as already noted above and, as we speculate, for the disorder in the distribution of ions (oxygen and titanium ions). In the case of $A(B'_{1-x}B''_x)O_3$ perovskites with ferroelectrically active cations in the B sublattice, as the difference in the length of the unstressed cation–cation bonds $\Delta L_B = |L_{B'} - L_{B''}|$ (or the difference in the radii) of the B′ and B″ cations increases, the relative displacement of the oxygen ions from the basal A planes increases, so that, the broadening of the transition increases as well [30].

When, the ferroelectrically active Ti cation is replaced by Sn in $BaTiO_3$, the degree of broadening increases monotonically with the concentration of Sn. The composition fluctuations denote the compositionally disordered ions or the existence of vacancies, interstitial ions, dislocations, and other defects. The influence of the degree of compositional disorder on the average transition temperature can be attributed to the disorder-related variation of the average diameter of the oxygen octahedra surrounding ferroelectric ions in the perovskite structure.

Since no impurity phases were observed in XRD and no elements other than Ba, Ti, Sn and O were detected by EDX (not shown here) for our SPS BTS_{13} pellets, the dielectric properties of the samples must be associated with the oxygen deficiency and nonuniform internal stresses due to these oxygen deficiencies. The oxygen deficiency creates disequilibrium of the charge in the ceramics. It can be compensated via the formation of Ti^{3+} and/or the presence of Ti vacancies (for electroneutrality), in the BTS_{13} sintered by SPS technique.

Based on these considerations, the value of Curie temperature, higher than that indicated in literature [10,11], can be attributed to partial reduction of Ti^{4+} to Ti^{3+} and to chemistry imbalances and defects created by SPS through the mechanisms mentioned in Section 1. Strongly suppressed grain growth in the SPS process may suggest that SPS influences in the first instance inter-grain regions. However, this affects further the grains at least due to newly occurred situation for oxygenation (in situ or post annealing). Such scenario, although it required further confirmation through detailed systematic experiments, can give an explanation for somehow different results obtained for the SPS-BTS_{13} ceramic when compared to conventional BTS_{13}. Results also indicate that refinement of the processing is highly desired and that SPS can play a positive role in controlling material's characteristics.

5. Conclusions

We used spark plasma sintering method for a fast pressing-sintering process of barium titanate stanate powders at 1200 °C, 10 min. Then, the pellets were annealed in oxygen, 5 h at 1100 °C. The as-obtained pellets consist of submicron grains. Final ceramic had a density of about ~99% of the theoretical one. The dielectric properties as a function of temperature and frequency, were from $\varepsilon_r = 5680$ and $\tan\delta = 0.009$ at Curie temperature $T_c = 57$ °C and 1 kHz to $\varepsilon_r = 5200$ and $\tan\delta = 0.004$ at 100 kHz and $T_c = 64$ °C. The dielectric maximum and the Curie temperature shifted to higher temperature for a higher frequency. The SPS manufactured $BaTi_{0.87}Sn_{0.13}O_3$ ceramics shown also a good tunability and ferroelectric properties. The differences in properties of our samples and conventionally processed ones presented in literature suggest that SPS can be a useful technique expanding the possibilities for the properties control of the BTS_{13} ceramic. This might be related to Ti/Sn (reduction of Ti^{4+} to Ti^{3+}) and/or oxygen behaviour and also to the defects. Further research is required.

Acknowledgements

We would like to gratefully acknowledge P. Badica for very useful and profitable discussions.

This research was supported by the "Nucleu"-project, PN09-450102, from the National plan for RDI, funded by the Romanian Ministry of Education and Research, and the National Authority for Scientific Research.

References

[1] E.C. Subbarao, Ferroelectrics 35 (1981) 143–148.
[2] R. Vivekanandan, T.R.N. Kutty, Ceram. Int. 14 (1988) 207–216.
[3] R. Wernicke, Ber. Dtsch. Keram. Ges. 55 (1978) 356–358.
[4] H. Brauer, Z. Angew. Phys. 29 (1970) 282–287.
[5] X. Wei, Y. Feng, L. Huang, S. Xia, L. Jin, X. Yao, Mater. Sci. Eng. B 120 (2005) 64–67.
[6] C.K. Campbell, J.D. van Wyck, M.F.K. Holm, J.J. Schoeman, IEEE Trans. Comp. Hybrid. Manuf. Technol. 15 (1992) 245–251.
[7] C.K. Campbell, J.D. van Wyck, M.F.K. Holm, J.J. Prinsloo, J.J. Schoeman, IEEE Trans. Comp. Hybrid. Manuf. Technol. 16 (1993) 418–423.
[8] S. Markovic, M. Mitric, N. Cvjeticanin, D. Uskokovic, J. Eur. Ceram. Soc. 27 (2007) 505–509.
[9] G.A. Smolensky, J. Phys. Soc. Japan 28 (1970) 26–37.
[10] N. Yasuda, H. Ohwa, S. Asano, Jpn. J. Appl. Phys. 35 (1996) 5099–5103.
[11] K. Oh, K. Uchino, L.E. Cross, J. Am. Ceram. Soc. 77 (1994) 2809–2816.
[12] J.-H. Jeon, Y.-D. Hahn, H.-D. Kim, J. Eur. Ceram. Soc. 21 (2001) 1653–1656.
[13] W. Xiaoyong, F. Yuju, Y. Xi, Appl. Phys. Lett. 83 (2003) 2031–2033.
[14] X. Wei, X. Yao, Mater. Sci. Eng. B 137 (2007) 184–188.
[15] V. Mueller, H. Beige, H.-P. Abicht, Appl. Phys. Lett. 84 (2004) 1341–1343.
[16] K.R. Anderson, J.R. Groza, M. Fendorf, C.J. Echer, Mater. Sci. Eng. A: Struct. Mater.: Properties, Microstruct. Process. A270 (2) (1999) 278–282.
[17] S.H. Risbud, J.R. Groza, M.J. Kim, Phil. Mag. 69 (1994) 525–533.
[18] Z.A. Munir, U. Anselmi-Tamburini, M. Ohyanagi, J. Mater. Sci. 41 (2006) 763–777.
[19] Z. Valdez-Nava, S. Guillemet-Fritsch, Ch. Tenailleau, T. Lebey, B. Durand, J.Y. Chane-Ching, J. Electroceram. 22 (2009) 238–244.
[20] T. Takeuchi, Y. Suyama, D.C. Sinclair, H. Kageyama, J. Mater. Sci. 36 (2001) 2329–2334.
[21] B. Li, X. Wang, M. Cai, L. Hao, L. Li, Mater. Chem. Phys. 1 (2003) 173–180.
[22] M. Cernea, D. Piazza, A. Manea, E. Vasile, C. Galassi, J. Am. Ceram. Soc. 90 (2007) 1728–1732.

[23] D.W. Richerson, in: W. David, Richerson (Eds.), Modern Ceramic Engineering: Properties, Processing, and Use in Design, 2nd ed., rev. and expanded, Marcel Dekker, Inc., New York, 1992, p. 128.
[24] R.H. Buttner, E.N. Maslen, Acta Crystallogr. Sec. B: Struct. Sci. 48 (1992) 764–769.
[25] L. Geske, V. Lorenz, T. Muller, L. Jager, H. Beige, H.-P. Abicht, V. Müller, J. Eur. Ceram. Soc. 25 (2005) 2537–2542.
[26] H.B. Sharma, H.N.K. Sarma, A. Mansingh, J. Mater. Sci. 34 (1999) 1385–1390.
[27] O.E. Kvyatkovskii, F. Karadag, A. Mamedov, G.A. Zakharov, Solid Phys. 46 (2004) 1663–1667.
[28] V.A. Isupov, Ferroelectrics 90 (1989) 113–118.
[29] V.A. Isupov, Ferroelectrics 143 (1993) 109–115.
[30] A.A. Bokov, JETP 84 (1997) 994–1002.